Pharmacological Research 167 (2021) 105548

Contents lists available at ScienceDirect

Pharmacological Research

journal homepage: www.elsevier.com/locate/yphrs

Resveratrol-mediated attenuation of superantigen-driven acute respiratory distress syndrome is mediated by microbiota in the lungs and gut

Hasan Alghetaa [1], Amira Mohammed [1], Juhua Zhou, Narendra Singh, Mitzi Nagarkatti, Prakash Nagarkatti [*]

Department of Pathology, Microbiology and Immunology, University of South Carolina School of Medicine, Columbia, SC 29208, USA

ARTICLE INFO

Keywords:
ARDS
Cytokine storm
Resveratrol
Superantigen
SEB
Microbiota

Chemical compounds studied in this article:
resveratrol (PubChem CID: 445154)
carboxymethylcellulose (PubCID: 24748)
interleukin 1beta (PubChem CID: 159483)
$DiOC_6(3)$ (3,3′-Dihexyloxacarbocyanine iodide, PubChem CID: 9894321)
lipopolysaccharide (LPS, PubChem CID: 451715)
metronidazole (Bioxtra, PubChem CID: 24896667)
butyric acid (PubChem CID: 264)
propionic acid (PubChem CID: 1032)
iso butyric acid (PubChem CID: 6590) and
acetic acid (PubChem CID: 176)

ABSTRACT

Acute Respiratory Distress Syndrome (ARDS) is triggered by a variety of agents, including Staphylococcal Enterotoxin B (SEB). Interestingly, a significant proportion of patients with COVID-19, also develop ARDS. In the absence of effective treatments, ARDS results in almost 40% mortality. Previous studies from our laboratory demonstrated that resveratrol (RES), a stilbenoid, with potent anti-inflammatory properties can attenuate SEB-induced ARDS. In the current study, we investigated the role of RES-induced alterations in the gut and lung microbiota in the regulation of ARDS. Our studies revealed that SEB administration induced inflammatory cytokines, ARDS, and 100% mortality in C3H/HeJ mice. Additionally, SEB caused a significant increase in pathogenic Proteobacteria phylum and *Propionibacterium acnes* species in the lungs. In contrast, RES treatment attenuated SEB-mediated ARDS and mortality in mice, and significantly increased probiotic Actinobacteria phylum, Tenericutes phylum, and *Lactobacillus reuteri* species in both the colon and lungs. Colonic Microbiota Transplantation (CMT) from SEB-injected mice that were treated with RES as well as the transfer of *L. reuteri* into recipient mice inhibited the production of SEB-mediated induction of pro-inflammatory cytokines such as IFN-γ and IL-17 but increased that of anti-inflammatory IL-10. Additionally, such CMT and *L. reuteri* recipient mice exposed to SEB, showed *a* decrease in lung-infiltrating mononuclear cells, cytotoxic CD8+ T cells, NKT cells, Th1 cells, and Th17 cells, but an increase in the population of regulatory T cells (Tregs) and Th3 cells, and increase in the survival of mice from SEB-mediated ARDS. Together, the current study demonstrates that ARDS induced by SEB triggers dysbiosis in the lungs and gut and that attenuation of ARDS by RES may be mediated, at least in part, by alterations in microbiota in the lungs and the gut, especially through the induction of beneficial bacteria such as *L. reuteri*.

1. Introduction

Acute respiratory distress syndrome (ARDS) is a form of respiratory failure that is triggered by a variety of stimuli such as pneumonia, sepsis, trauma, and certain viral infections. Typically, ARDS results from hyperactivation of the immune response leading to heightened inflammation in the lungs followed by the development of pulmonary edema, alveolar damage, and respiratory failure [1]. More than 200,000 people suffer from ARDS annually in the USA and over 3 million people globally. ARDS causes over 75,000 deaths in the USA alone, with over 37.5% mortality [1]. Because a significant proportion of COVID-19 patients develop ARDS, this clinical disorder is on the rise and currently, there are no FDA-approved drugs to treat ARDS.

ARDS usually induces damage of vascular endothelium and alveolar epithelium, transepithelial migration of neutrophils and T cells, and release of pro-inflammatory cytokines such as IL-1β, IL-6, IFN-γ, and tumor necrosis factor-alpha (TNF-α)) and cytotoxic mediators [2–4]. While ARDS is associated with hyperactivation of the immune system

Abbreviations: ABX, antibiotic mixture; ARDS, acute respiratory distress syndrome; CMT, colonic material transplant; IL, interleukin; L. reuteri, Lactobacillus reuteri; MNCs, mononuclear cells; NKT, natural killer T lymphocytes; OTUs, operational taxonomic units; QIIME, Quantitative Insights Into Microbial Ecology; SCFAs, short chain fatty acids; SEB, staphylococcal enterotoxin-B; Th1, T helper-1; Th17, Thelper-17; Th3, T helper-3; Tregs, T regulatory cells.

[*] Correspondence to: University of South Carolina, 202 Osborne Administration Building, Columbia, SC 29208, USA.
E-mail address: prakash@mailbox.sc.edu (P. Nagarkatti).
[1] The current affiliation is Department of Veterinary Physiology, Pharmacology and Biochemistry, College of Veterinary Medicine, University of Baghdad. Baghdad - Iraq.

https://doi.org/10.1016/j.phrs.2021.105548
Received 4 August 2020; Received in revised form 23 February 2021; Accepted 9 March 2021
Available online 15 March 2021

and cytokine storm, the precise nature of the trigger remains unclear. However, with SEB-mediated ARDS, it is clear that SEB acts as a superantigen and triggers a large proportion of T cells bearing certain Vβ specificities, leading to cytokine storm [5–7].

Resveratrol (RES), 3, 4′, 5 trihydroxy stilbene, is a naturally occurring polyphenol present in grapes, berries, and peanuts [8,9]. RES has antioxidant, anti-inflammatory, and anticancer properties [8,10]. Therefore, resveratrol may play a role in the prevention of cancer, cardiovascular, and autoimmune diseases [8,11]. Our previous studies discovered that resveratrol could inhibit the severity of ARDS and asthma in mice [12–14]. The underlying mechanisms include the ability of RES to significantly increase apoptosis in activated T cells, attenuation of inflammatory cytokine production, and augmented induction of Cd11b+ and Gr1+ myeloid-derived suppressor cells [12]. In addition, resveratrol significantly altered the expression of microRNAs (miRNAs) in the immune cells isolated from the lungs of ARDS mice. Particularly, RES significantly down-regulated the expression of miR-193a, which targeted several molecules involved in TGF-β signaling and activation of apoptotic pathways death receptor-6 [13].

It has been shown that microbiota may play an important role in disease pathogenesis [15–17]. It has been reported that lung and gut microbiota are associated with the development, regulation, and maintenance of healthy immune responses and the regulation of lung diseases such as asthma and allergy [18–20]. Thus, microbiota may also play a role in the regulation of ARDS [17, 21, 22]. Recent studies have shown that RES may markedly alter gut microbiota [23,24]. However, the functions of RES in the regulation of lung and gut microbiota associated with ARDS are unknown.

SEB, produced by Staphylococcus aureus, a ubiquitous, gram-positive bacterium is the prototype superantigen that triggers cytokine storm, and inhalation of SEB leads to toxic shock syndrome, respiratory failure, and often death [25]. Thus, SEB-induced lung injury is a good model for investigating the mechanism of ARDS pathogenesis [12]. In this study, we investigated whether the ability of RES to attenuate ARDS results from alterations in the microbiota in the lungs and gut. Our studies demonstrate that RES does alter the microbiota in SEB-exposed mice and furthermore CMT experiments conclusively demonstrate that RES-induced microbiota, specifically, *L. reuteri* plays a significant role in the attenuation of ARDS.

2. Materials and methods

2.1. Experimental animals

C3H/HeJ female mice were purchased from Jackson laboratory at age of 6 weeks and housed in specific pathogen-free (SPF) conditions for 1–2 weeks before performing any experiments. Animal housing and use were approved by the University of South Carolina Institutional Care and Use Committee (IACUC) under AUP 2363 according to the guidelines of the Care and Use of Laboratory Animals of the National Research Council.

2.2. Animals grouping and housing

All delivered mice were kept for one week as an acclimatization period prior to any experiment performed. Animals were housed in a maximum of 5 mice per cage under an equal ratio of light to dark at a temperature of ~18–23 °C and 40–60% humidity. Food and water were available ad libitum. To minimize the microbiome variations from cage/rack to cage/rack due to managerial and housekeeping effects, experimental mice were selected randomly from different 5 cages to house them in one new cage in a maximum number of 5 mice/cage, and then each cage was blindly assigned for different treatments or kept as control group according to the experimental design.

2.3. SEB administration

SEB (Toxin Technology, Sarasota, FL, USA) was used in the induction of ARDS as a dual dose, which is known to cause ARDS and 100% mortality, described previously [26]. Briefly, mice were randomized and 5 μg/mouse of SEB was administrated intranasally in isoflurane-anesthetized mice, and then returned to special biohazardous cages. After 120 min of the first SEB administration, mice received the second dose of SEB by the intraperitoneal route in the dose of 2 μg/mouse SEB.

2.4. RES administration

RES (Supelco, Millipore-Sigma, St. Louis, MO, USA) was used in SEB-mediated ARDS as detailed elsewhere [12,13]. Mice received two doses of 100 mg/kg mouse body weight of RES suspended in 1% Carboxymethylcellulose (CMC, Millipore-Sigma, St. Louis, MO, USA) by oral-gavage at 24 h, and 90 min prior to the administration of the SEB dose. 1% Carboxymethylcellulose was used as vehicle control (VEH). All mice were kept in autoclaved cages and placed in the separated-housing room for incubating hazard-agent-exposed animals.

2.5. Sample collection

After 48 h of the second SEB-dose administration, mice were euthanized with >5% isoflurane (Zoetis, Parsippany, NJ, USA) in a saturated chamber for sample collection. Blood was collected from each mouse and serum was separated. Lung tissues were harvested and used in the analysis of lung-infiltrating mono-nuclear cells (MNCs) and microbiota profiles as described by us previously [13,27].

2.6. Mononuclear cell (MNC) isolation and T cell subset determination from lungs and spleen

Lung-infiltrating MNCs and splenocytes were prepared as described previously [13]. The isolated cells were stained in the fluorescence-activated cell sorting (FACS) buffer containing different specific fluorochrome-conjugated antibodies including BV510-conjugated interleukin-17 (IL-17) antibody, BV650-conjugated interferon-gamma (IFN-γ) antibody, BV785-conjugated CD3 antibody, Alexa Fluor 488-conjugated FoxP3 antibody, PE-conjugated IL-10 antibody, PE-CF594-conjugated NK1.1 antibody, PE-Cy5.5-conjugated transforming growth factor-beta (TGF-β) antibody, Alexa Fluor 647-conjugated IL-4 antibody, Alexa Fluor 700-conjugated CD8 antibody and APC-Cy7-conjugated CD4 antibody (Biolegend, San Diego, CA, USA) to determine the T cell subset populations. Cellular membrane and nuclear membranes were permeabilized by using Fixation/Permeabilization Solution Kit (BD, Franklin Lakes, NJ, USA) and True-nuclear Transcription Factor Buffer Set (Biolegend, San Diego, CA, USA), respectively. Then stained cells were suspended in FACS buffer and analyzed in BD-FACS Celesta flow cytometry system (BD, Franklin Lakes, NJ, USA). Acquired data were further analyzed using Diva software or FlowJo V10 software (BD, Franklin Lakes, NJ, USA). Isotype controls were used to identify the positive population (Fig. 1).

2.7. Cytokine measurement

The concentrations of cytokines including IL-1β, IL-10, IL-17 and IFN-γ in the serum samples from mice after 48 h of SEB administration were measured by enzyme-linked Immunosorbent Assay (ELISA), as detailed elsewhere [28] using commercial mouse-specific cytokine ELISA kits (Biolegend, San Diego, CA, USA) according to the manufacturer's instructions. The concentrations of cytokines were determined by measuring the absorbance at 450 nm wavelength using a Victor 2 plate reader (Perkin Elmer, Hopkinton, MA, USA). Expression of IFN-γ gene in lung-infiltrating MNCs was also determined by real-time polymerase

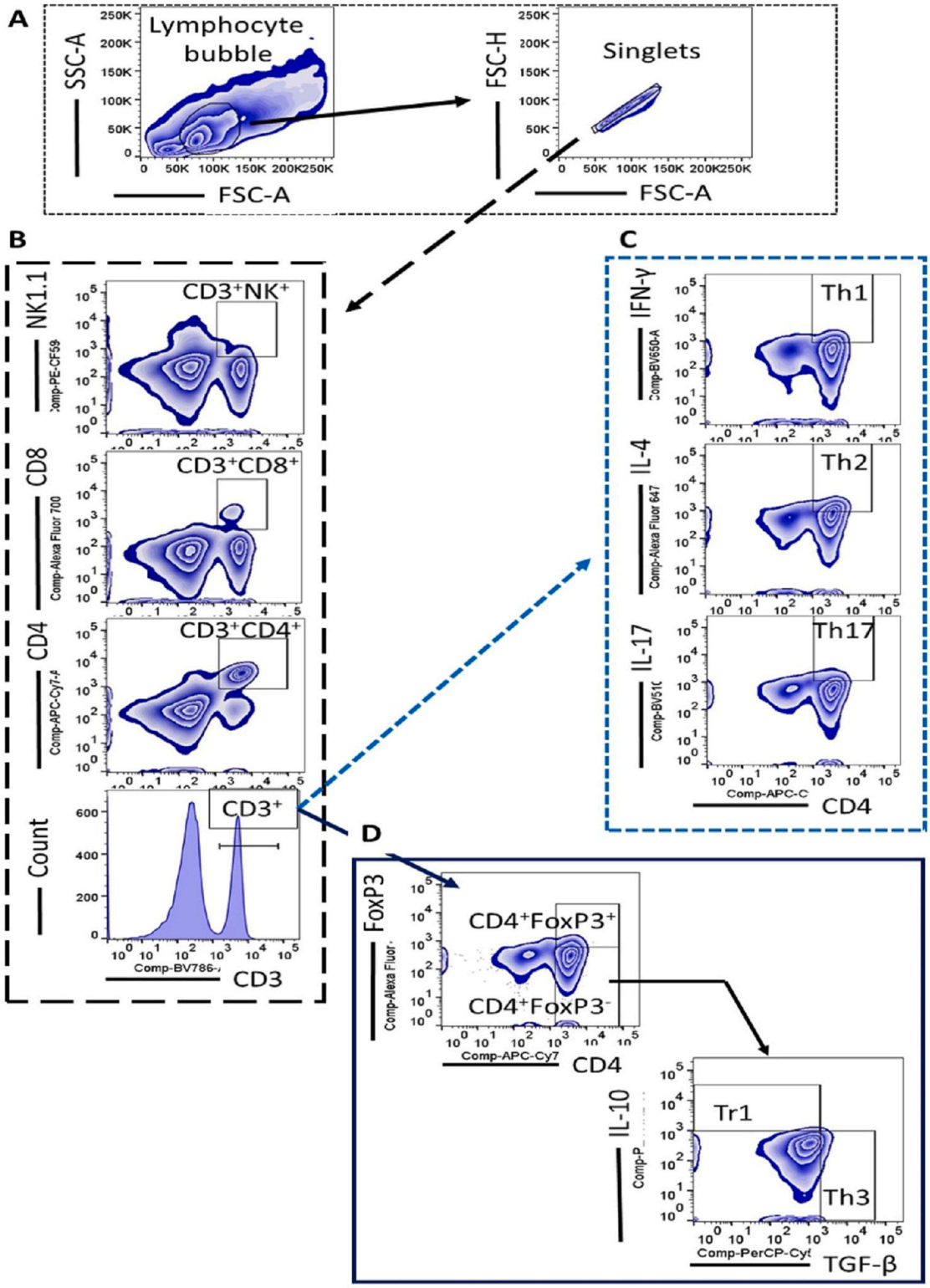

Fig. 1. Gating strategy of multi-parametric flow-cytometry analysis of T-lymphocyte subsets. A) Discrimination of lymphocytes and singlets. B) Major T cell components, from top; $CD3^+NK1.1^+$ (NKT), $CD3^+CD8^+$ (CTL), $CD3^+CD4^+$ cells and histogram of $CD3^+$ cells population. C) T-helper subsets gated on $CD3^+$ cells; from top $CD4^+IFN\text{-}\gamma^+$ (Th1), $CD4^+IL4^+$ (Th2) and $CD4^+IL17^+$ (Th17). D) T regulatory cells and $FoxP3^-$ T-reg (upper panel) and $FoxP3^-$ Treg subsets, $IL10^+$ cells (Tr1) or $TGF\text{-}\beta^+$ cells (Th3). NKT: natural killer T cells; CTL: cytotoxic T lymphocytes; Th: T helper lymphocytes; Tr1: T regulatory cells type-1.

chain reaction (qPCR), as described [13].

2.8. Bacterial DNA extraction from the lungs

In highly aseptic environments, DNA samples including bacterial DNA was isolated from lung tissues according to the instruction manual

of Quick-DNA Fungal/Bacterial MidiPrep Kit (Zymo Research Corp, Irvine, CA, USA) according to the manufacturer's protocol. In brief, lung tissues were placed in a Bashing Bead lysis/filtration tube with 6 ml of Fungal/bacterial DNA binding buffer, shaken vigorously for about 1 min, and then centrifuged for 3 min at room temperature. Using Zymo-spin V-E Column/Zymo-midi filter, the entire mixture of buffer filtrate was filtered by spanning for 1 min and lastly, the columns were assembled to new collection tubes, washed with DNA Pre-wash Buffer, and DNA solution was eluted with 150 µl of DNA Elution Buffer.

2.9. Colon content preparation

Colonic content was collected aseptically for isolating gut-bacterial DNA and measuring the concentrations of short-chain fatty acids (SCFAs), as described [23]. Briefly, colonic segments were excised from mice and transferred into a sterile 12-well plate containing 1 ml of sterile PBS per well to minimize the exposure of anaerobic bacteria to oxygen. Then, PBS-immersed segments were opened longitudinally to remove the contents with a disposable sterile scraper, and the contents were collected in sterile tubes and stored in −80 °C for further use.

2.10. Identification and quantification of short chain fatty acids (SCFA)

SCFA were detected as described [23]. Briefly, colonic contents were suspended in water. After centrifugation, the supernatants were saved and acidified by HCl. 4-methylvaleric acid was used as an internal standard. SCFAs were identified and quantified by the gas chromatograph CP-3800 (Varian) and mass spectrometry (GC-MS) system [30]. Varian MS Workstation (version 6.9.2.) software was used to collect and analyze the data. The linear regression equation was used to calculate the concentrations of specific SCFAs in colon samples.

2.11. Bacterial DNA extraction from colon contents

In a highly aseptic environment, bacterial DNA samples were isolated from flushed colonic contents using QIAamp DNA Stool Mini Kit (Qiagen, Germantown, MD, USA). Based on the instruction manual, the first step was modified by increasing the lysate temperature to 95 °C instead of 70 °C to break down the hard-cellular wall of Gram-positive bacteria to ensure the release of bacterial DNA. The isolated DNA samples were quantified using Qubit 3.0 fluorimeter (Invitrogen, ThermoFisher Scientific, Waltham, MA, USA) and stored at −80 °C for the use in 16S metagenomics library preparation and qPCR validation, as detailed elsewhere [30].

2.12. Analysis of microbiota by pyrosequencing

Lung and gut microbiota were analyzed by pyrosequencing as detailed elsewhere [31]. DNA samples from lung tissues and colon contents were used in the preparation of 16S ribosomal RNA gene amplicons. According to Illumina protocol of 16S Metagenomic Sequencing Library Preparation, amplification of the 16S ribosomal RNA V3-V4 hypervariable regions were carried out by PCR using the primers designed and tested by Klindworth et al. [32]. The sequence of 16S Amplicon PCR Forward Primer was 5′-TCGTCGGCAGCGTCAGATGTGTATAAGAGACAGCCTACGGGNGGCWG CAG-3′, and that of 16S Amplicon PCR Reverse Primer was 5′- GTCTCGTGGGCTCGGAGA TGTGTATAAGAGACAGGACTACHVGGGTATCTAATCC-3′. Each reaction mixture (25 µl) contained 12.5 ng DNA isolated from lung tissues or colon contents, 0.2 µM amplicon PCR forward primer, 0.2 µM amplicon PCR reverse primer and KAPA HiFi HotStart Ready Mix. PCR was performed in Bio-Rad thermal cycler as the initial step of 95 °C for 3 min, the second step of 25 cycles of 95 °C for 30 s, 55 °C for 30 s and 72 °C for 30 s, and a final extension step at 72 °C for 5 min. After PCR amplification, each reaction was cleaned up using Agencourt AMPure XP beads on the magnetic field to purify the 16S ribosomal RNA V3 and V4 amplicons. Then, the sizes of produced amplicons were determined by gel electrophoresis, and the desired amplicon size was 550 bp.

Illumina dual indices were added to the 16S ribosomal RNA gene amplicons by PCR. Each reaction mixture consisted of 5 µl 16S ribosomal RNA gene amplicons, 5 µl Illumina Nextera XT Index Primer 1 (N7xx), 5 µl Nextera XT Index Primer 2 (S5xx), 25 µl 2 × KAPA HiFi Hot Start Ready Mix, and 10 µl PCR-grade water. PCR was carried out in Bio-Rad thermal cycler as the initial step of 95 °C for 3 min, the second step of 8 cycles of 95 °C for 30 s, 55 °C for 30 s and 72 °C for 30 s, and a final extension step at 72 °C for 5 min. Then, the constructed 16S metagenomic libraries were purified with Agencourt AMPure XP beads and quantified using Quant-iTPicoGreen. The quality and size distribution of constructed libraries were determined using the Agilent Technologies 2100 Bioanalyzer. The libraries were normalized and pooled to 4 nM based on the quantified values. The pooled library samples were denatured and diluted to a final concentration of 8pM with a 25% PhiX control (Illumina, San Diego, CA, USA). The amplicons in the pooled library samples were subjected to pyrosequencing using the MiSeq Reagent Kit v3 in the Illumina MiSeq System for 600 cycles, which took around 56 h to generate about 100 K reads per sample.

After pyrosequencing, sequencing data collected from the Illumina Miseq system in FASTQ files along with map file in excel format were uploaded to the online 16S analysis platform, Nephele (https://nephele.niaid.nih.gov/) [33], supported by the Office of Cyber Infrastructure and Computational Biology (OCICB), National Institute of Allergy and Infectious Diseases (NIAID), NIH. The 16S metagenomics was analyzed through 16S Paired-end QIIME method, the groups of related DNA sequences were assigned to operational taxonomic units (OTUs), and Nephele-generated output pipeline files were analyzed to determine targeted tissue-microbial compositions. The default setting of Nephele was excluding any samples with the median OUT less than 0.2 OTU fractions of the highest sample in the same run in order to increase the quality of the reads, and then the generated FASTA files were blasted into Greengenes_99 database at 70% cutoff similarity.

2.13. qPCR validation of L. reuteri bacterial abundance

DNA samples from lung tissues and colon contents were used to validate the abundance of *L. reuteri* bacterium in different biological samples by qPCR detection of *L. reuteri* DSM 20016 16S ribosomal RNA gene (NCBI accession No. NR_119069.1) expression. The sequence of forward primer of *L. reuteri* 16S ribosomal RNA gene was 5′-GACTTGAGTGCAGAAGA GGACA-3′, and that of reverse primer was 5′-CTGTTCGCTACCCATGCTTTC-3′. Using the delta-delta-CT method, the expression of a eubacteria 16S ribosomal RNA gene was used to normalize the relative expression of *L. reuteri* 16S ribosomal RNA gene as fold changes. The sequence of forward primer of the eubacteria 16S ribosomal RNA gene was 5′- ACTCCTACGGGAGGCAGCAGT -3′, and that of reverse primer was 5′- ATTACCGCGGCTGCTGGC -3′. SsoAdvanced Universal SYBER Green Supermix (Bio-Rad, Hercules, CA, USA) was used in qPCR detection of 16S ribosomal RNA genes according to the manufacture manual. qPCR was carried out in CFX384 Touch Real-Time PCR Detection System (Bio-Rad) as the initial step of 98 °C for 10 s, the second step of 40 cycles of 98 °C for 10 s and 60 °C for 30 s, and the final step of melt curve analysis according to the instruction protocol.

2.14. Preparation of Lactobacillus reuteri cells for transfer experiments

Bacterial strain *Lactobacillus reuteri* was purchased from American Type Culture Collection (ATCC, Manassas, VA) under deposited name *Lactobacillus fermentum* Beijerinck (ATCC23272). Based on the vendor recommendation, the frozen bacterial cells were cultured aerobically in Difco™ Lactobacilli MRS Broth (BD, San Jose, CA, USA) at 37 °C for 24 h. Cultured *L. reuteri* bacterial cells were harvested at the mid-log phase of growth, spun down at 2000 g at 25 °C for 5 min, washed with sterile PBS twice, suspended in sterile PBS and used to transfer into

mice exposed to SEB. At the same time, the supernatant was saved, purified using 0.2 μm filter, and stored at −80 °C for further use as raw bacterial metabolites (named as the total culture metabolite, TCM). Mice received the oral dose of 2×10^{10} bacterial cells/mouse per day for 5 consecutive days prior to SEB administration.

2.15. Microbiota depletion and mouse treatment for CMT studies

In order to deplete the endogenous microbiota, mice were treated for 4 weeks with the extensive antibiotic mixture (ABX) as described [34], containing 250 mg/ml bacitracin, 170 μg/ml gentamycin, 125 μg/ml ciprofloxacin, 100 μg/ml neomycin, 100 μg/ml metronidazole, 100 μg/ml ceftazidime, 100 U/ml penicillin, 50 μg/ml streptomycin and 50 μg/ml vancomycin (MilliporeSigma, St. Louis, MO, USA), supplemented with 1 g/L sweetener (Splenda, Carmel, IN, USA) to overcome the metallic taste of the mixture in drinking water. Fecal pellets were collected from different groups of mice aseptically 3 days prior to the last day of ABX treatment for bacterial culture examination and qPCR validation of the eubacteria 16S ribosomal RNA gene expression. ABX-treated mice received the colonic content and were challenged with SEB dual dose, as described earlier. These mice were euthanized for lung tissue and colon content collection, hematological evaluation, lung-infiltrating MNC analysis, and gut microbiota profiling as described previously [13,27].

2.16. Colonic Microbiota Transplantation (CMT)

CMT was performed as detailed elsewhere [17,34]. Donor mice received Vehicle, RES, SEB + VEH or SEB + RES. Next, the colonic material was transferred into ABX-treated mice which were challenged with dual dose of SEB as described above. Briefly, donor mice were deeply anesthetized with isoflurane, euthanized through cervical dislocation and transferred into an anaerobic chamber filled with the mixture of 5% H_2 and 5% CO_2 balanced with N_2 gas (Praxair, Danbury, CT, USA) at 37 °C to open up mouse abdominal and peritoneal cavity to collect the colonic materials aseptically. Then, the colonic material was suspended in sterile PBS, and filtered with 100 μm strainer to remove any undigested materials. The filtered colonic material was pooled from individual mice, weighed and adjusted to the equal concentration among different donor groups. Finally, the adjusted and filtered colonic material was loaded into 1 ml tuberculin syringe attached with plastic gavage for transplant into recipient mice.

CMT from the donor mice into ABX-treated mice was designated as follows: CMT from vehicle-treated mice into ABX mice followed by SEB (VEH→SEB), CMT from RES-treated mice into ABX mice followed by SEB (RES→SEB), CMT from SEB + VEH treated mice into ABX mice followed by SEB (SEB + VEH→SEB), and CMT from SEB + RES treated mice into ABX mice followed by SEB (SEB + RES→SEB). In some experiments, *L. reuteri* was also transferred into ABX mice followed by SEB (*L. Reuteri* →SEB). After 48 h of the second SEB-dose administration, mice were euthanized for colonic material collection.

Recipient mice were treated with ABX for 4 weeks to deplete endogenous microbiota as described above, and then fed with autoclaved normal drinking water overnight. Next day, recipient mice were co-housed with the pre-treated donor mice at the ratio of 1:1 in donor mouse cages for 24 h. On the following day after donor-recipient mouse cohousing, donor mice were sacrificed for colonic material collection, and each recipient mouse received CMT from donor mice. Lastly, recipient mice received the administration of dual SEB doses. After forty-eight hours of SEB administration, mice were euthanized for the collection of different samples including blood, colon tissues, colonic contents, lung tissues and spleen, which were used in hematological evaluation, lung-infiltrating MNC analysis, and gut microbiota profiling as we described previously.

2.17. Assessment of mouse survival rates

After mice received different treatments and the second dose of SEB, mice were carefully monitored for survival. Any moribund mice were immediately euthanized.

2.18. Effect of SEB-activated immunocytes on the alveolar barrier function

Non-invasive real-time monitoring of the barrier function of lung epithelial cells type II (MLE15) was performed by using an electric cell-substrate impedance sensing z-theta (ECISzθ) system as described previously by our laboratory [7]. Briefly, MLE15 cells were seeded at a rate of 12×10^4 cells/well on gold-coated electrode arrays, 8W10E+ , up to being confluent and forming a monolayer of cells (~72 h) then co-cultured with SEB-activated splenocytes pre-treated with RES or VEH. The resistance of the monolayer cells was evaluated for 24 h after wounding the monolayer epithelial cells with treated splenocytes by using a multifrequency test (MFT) to find that 250 Hz was the optimum frequency to be used. The real-time resistance was measured for approximately 24 h in intervals of every two minutes post co-culturing the alveolar epithelial cells with SEB-activated splenocytes. A cell-free well was considered as a control, and the barrier resistance values were calculated after being normalized to the resistance of the cells before being wounded with activated splenocytes.

2.19. Mitochondrial membrane potential

To analyze the apoptotic effect of RES or VEH on the SEB-activated splenocytes, the mitochondrial membrane potential of whole lung-infiltrating mononuclear cells and T-cells ($CD3^+$ cells) was evaluated by using $DiOC_6$[3] dye uptake (ENZO Life Sciences, Farmingdale, NY) and flow cytometric analysis, as described by [7].

2.20. Statistical analysis

Statistical analysis was performed using GraphPad Prism 8 (GraphPad Inc, La Jolla, CA). Four to eight mice per group were used as determined by power analysis. The data shown in this study represent at least three independent experiments unless otherwise stated. Average values ± standard error mean (SEM) were presented for every parameter. The statistical differences between the two experimental groups were calculated using Student's t-test corrected by Holm-Sidak method for multiple comparisons. For comparisons of three or more groups, one-way ANOVA and Tukey's multiple comparisons post-hoc test was performed. Log-rank (Mantel-Cox) test was used to compare the survival curves. Mann-Whitney test was used to compare the significant changes in the curve of barrier function. A p value < 0.05 was considered significant for all experiments and different small letters were used to depict significant differences among various groups.

3. Results

3.1. Regulation of gut microbiota by RES in ARDS

Our previous studies revealed that the dual dose of SEB used in the current study causes ARDS and severe lung injury and that treatment with RES can attenuate the severity of ARDS [12, 13, 35]. It also has been reported that RES can modulate gut microbiota [23,24]. Thus, we tested if RES-mediated attenuation of SEB-mediated ARDS is associated with alterations in gut microbiota. To that end, we used three groups of mice: Naïve, SEB + VEH and SEB + RES and performed pyrosequencing of 16S bacterial ribosomal RNA genes to study the gut microbiota. The data showed that SEB triggered changes in the microbiota in the colon when compared to naïve mice and there were significant differences between SEB + VEH vs SEB + RES groups as shown in the principal

coordinate analysis (PCoA) plot (Fig. 2A). Specifically, SEB + RES treatment significantly increased the bacterial biomass in colon (Fig. 2B), augmented the abundance of phylum Tenericutes (Fig. 2D, E), increased the abundance of *Lactobacillus spp.* as shown in the cladogram (Fig. 2F), increased the population of *Lactobacillus reuteri* (Fig. 2F, G), and increased production of propionic acid, iso-butyric acid, and butyric acid (Fig. 2H), when compared to SEB + VEH. We did not see any difference in the Shannon Diversity Index between the groups (Fig. 2C). Together these data suggested that SEB induces dysbiosis in the gut and RES treatment alters the microbiota and SCFA, specifically, causing an increase in the abundance of *Lactobacillus spp.* such as *Lactobacillus reuteri* in gut microbiota.

3.2. Regulation lung microbiota dysbiosis associated with ARDS by RES

Next, we investigated if SEB alters the microbiota in the lungs and if RES treatment would reverse that. The data showed that SEB triggered changes in microbiota in the lungs and there were differences between the three groups (naïve mice, SEB + VEH and SEB + RES) as seen from distinct clusters shown in the principal coordinate analysis (PCoA) plot (Fig. 3A). SEB + VEH significantly increased the biomass of lung microbiota when compared to naïve mice and SEB + RES treatment

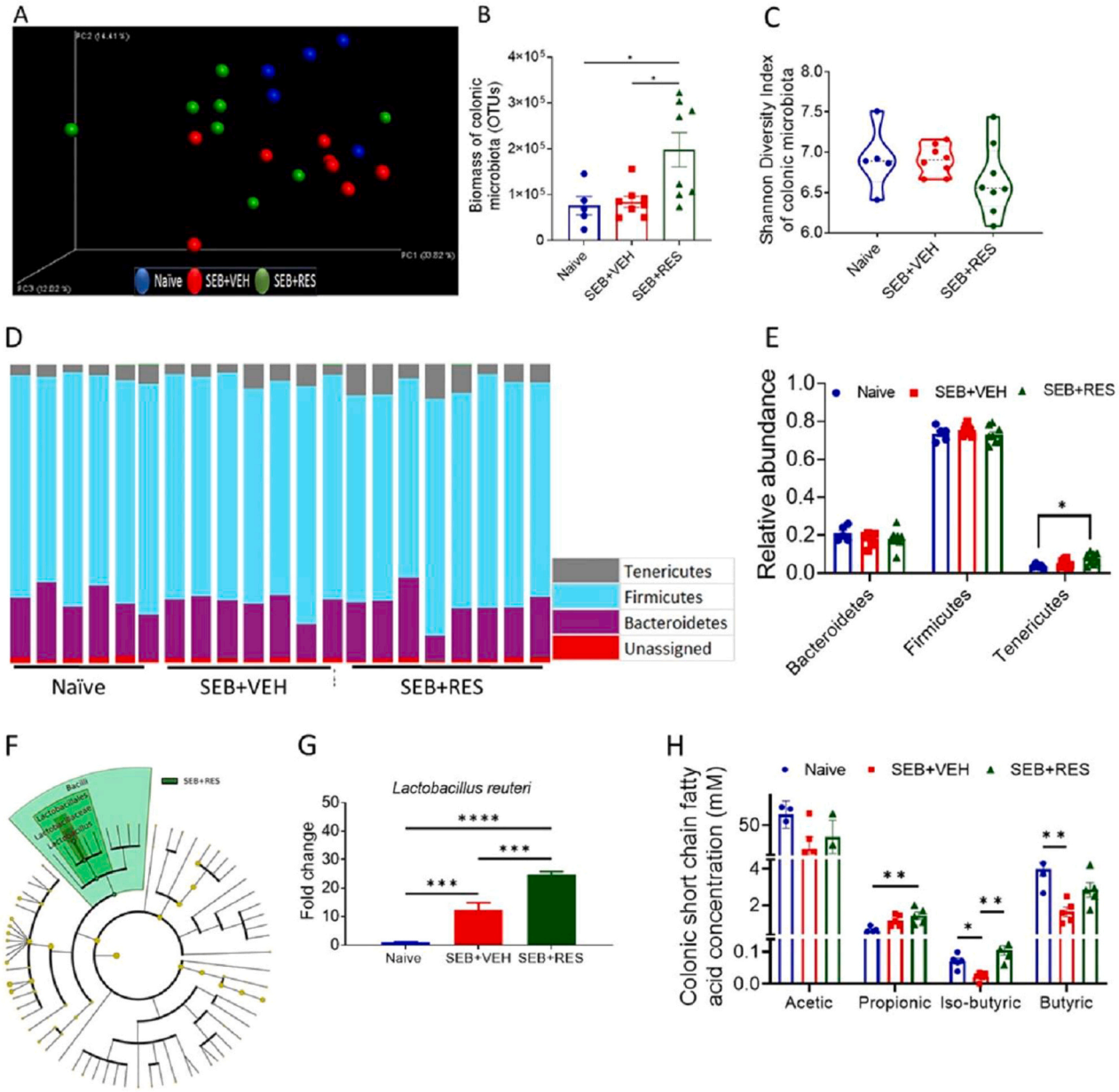

Fig. 2. Resveratrol treatment alters gut microbial composition and SCFA production in SEB-induced ARDS. Naïve mice or those treated with SEB + VEH or SEB + RES were studied for alterations in gut microbiota 48 h after SEB injection as described in Methods. A) Principal coordinate analysis plot reveals the clustering of individual commensal bacteria in colon based on their 16S rRNA content similarity. B) Comparison of bacterial biomass in the lung and colon represented by number of OTUs. C) Shannon index shows the diversity of microbiome in various groups in colonic lumen. D) Stack bar plot shows the relative abundance of major colonic bacterial phyla among experimental groups with statistical analysis. E) Comparison of abundance of bacteroidetes, firmicutes and tenericutes in colon. F) Cladogram generated from LEfSe analysis of taxonomic levels of colon microbiota shows biomarker bacteria between SEB + RES group when compared to SEB + VEH group. G) qPCR validation of *Lactobacillus reuteri* gene expression in isolated bacterial DNA from colons of experimental groups. H) Detection of SCFAs in the colon flushes measured by GC-FID technology. One-way ANOVA test was used and p-value < 0.05 is considered a significant difference. *$p < 0.05$, **$p < 0.01$, ***$p < 0.001$ and ****$p < 0.0001$.

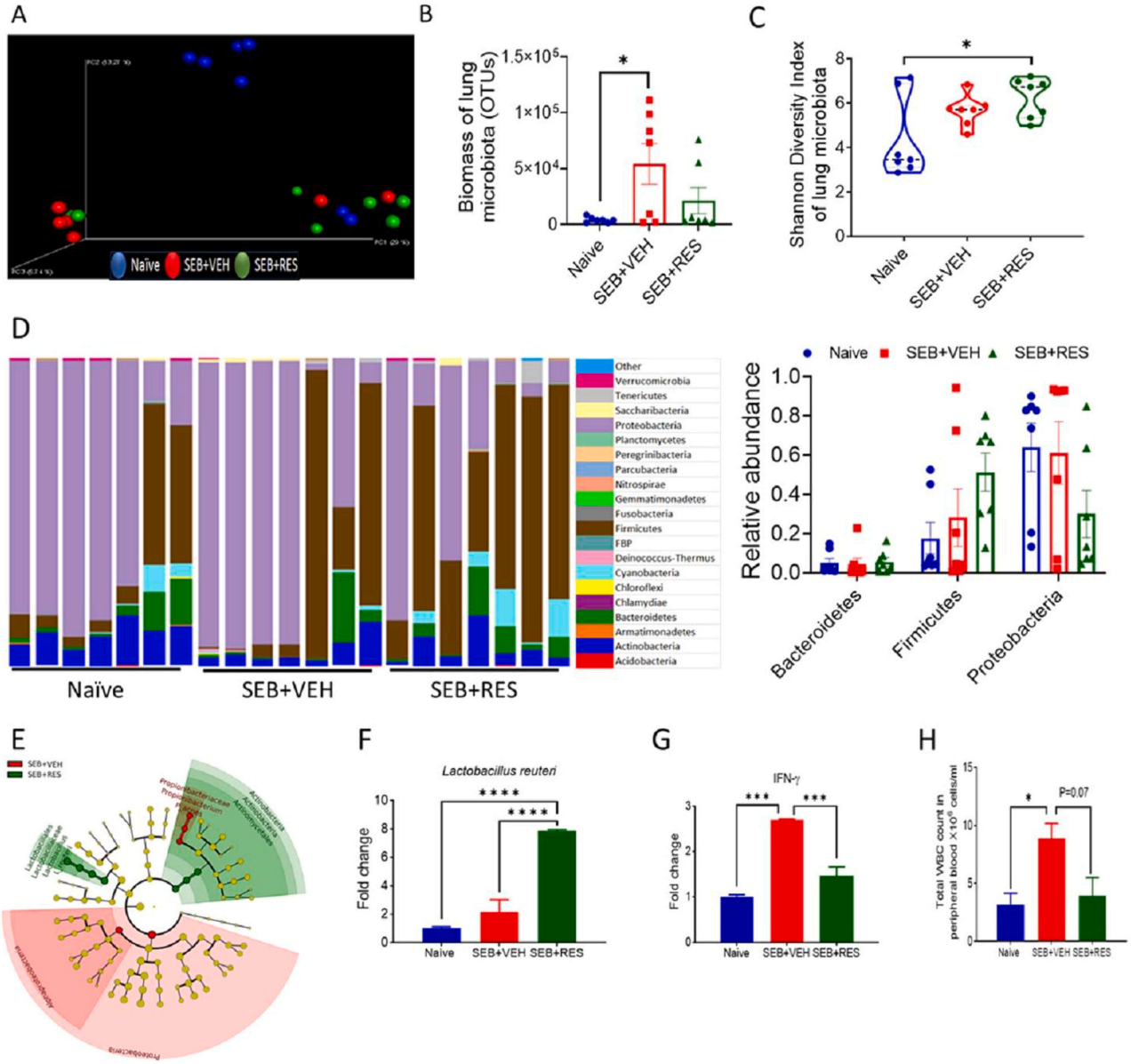

Fig. 3. Resveratrol treatment alters lung microbiota and increased enrichment of beneficial bacteria and suppression of SEB-mediated inflammation. Mice were treated with SEB + VEH or SEB + RES as described in Fig. 1 legend. A) Principal coordinate analysis plot reveals the clustering of individual commensal bacteria in the lungs based on their 16S rRNA content similarity. B) Comparison of lung bacterial biomass represented by abundance of OTUs. C) Shannon index shows the diversity of microbiome in lung tissue. D) Stack bar plot shows the fluctuations of major bacterial phyla among groups in lung tissue with statistical analysis of major enriched phyla (right panel). E) Cladogram depicting biomarkers between SEB-induced mouse group and both SEB-induced and RES-treated group. F) qPCR validation of *Lactobacillus reuteri* gene expression in isolated bacterial DNA from experimental groups. G) qPCR validation of pro-inflammatory gene, IFN-γ, in infiltrating mononuclear cells (MNCs) in lungs H) VetScan results show the systemic response in SEB exposure depicted by total number of white blood cells in peripheral blood of experimental mice. One-way ANOVA test was used and p-value < 0.05 is considered a significant difference. *$p < 0.05$, **$p < 0.01$, ***$p < 0.001$ and ****$p < 0.0001$.

decreased the biomass when compared to SEB + VEH group (Fig. 3B). Both SEB + VEH and SEB + RES groups showed significant alterations in the diversity of lung microbiota when compared to the naïve group (Fig. 3C) but no significant differences were seen in Bacteroidetes, Firmicutes and Proteobacteria (Fig. 3D). Furthermore, LEfSe (Linear discriminant analysis Effect Size) using Galaxy-LEfSe software [36] showed that the SEB + VEH group had increased the abundance of phylum Proteobacteria and species *Propionibacterium acnes*, whereas the SEB + RES group had increased the abundance of phylum Actinobacteria and species *Lactobacillus reuteri* (Fig. 3E). qPCR validation confirmed that the SEB + RES group had a significantly increased population of *Lactobacillus reuteri* in the lungs (Fig. 3F). Because SEB is a superantigen that triggers cytokine storm as shown previously by us [13, 35], we next checked for the expression of IFN-γ gene and found that in lung-infiltrating MNCs, expression of IFN-γ gene as well as the total number of white blood cells (WBC) in peripheral blood of SEB + VEH treated mice were significantly increased (Fig. 3G, H). In contrast, SEB + RES group had significantly decreased levels of IFN-γ gene and total number of WBC in peripheral blood (Fig. 3G, H). Additionally, SEB + RES treatment also caused a decrease in total numbers of lung infiltrating cells (Fig. 4A) and serum IFN-γ levels (Fig. 4B), a decrease in CD8+ cytotoxic T lymphocytes (CTL) and NKT cell numbers (Fig. 4C) but not percentage (Fig. 4D), while causing an increase in anti-inflammatory pathways such as Tregs (Fig. 4E), Th3 cells (Fig. 4F),

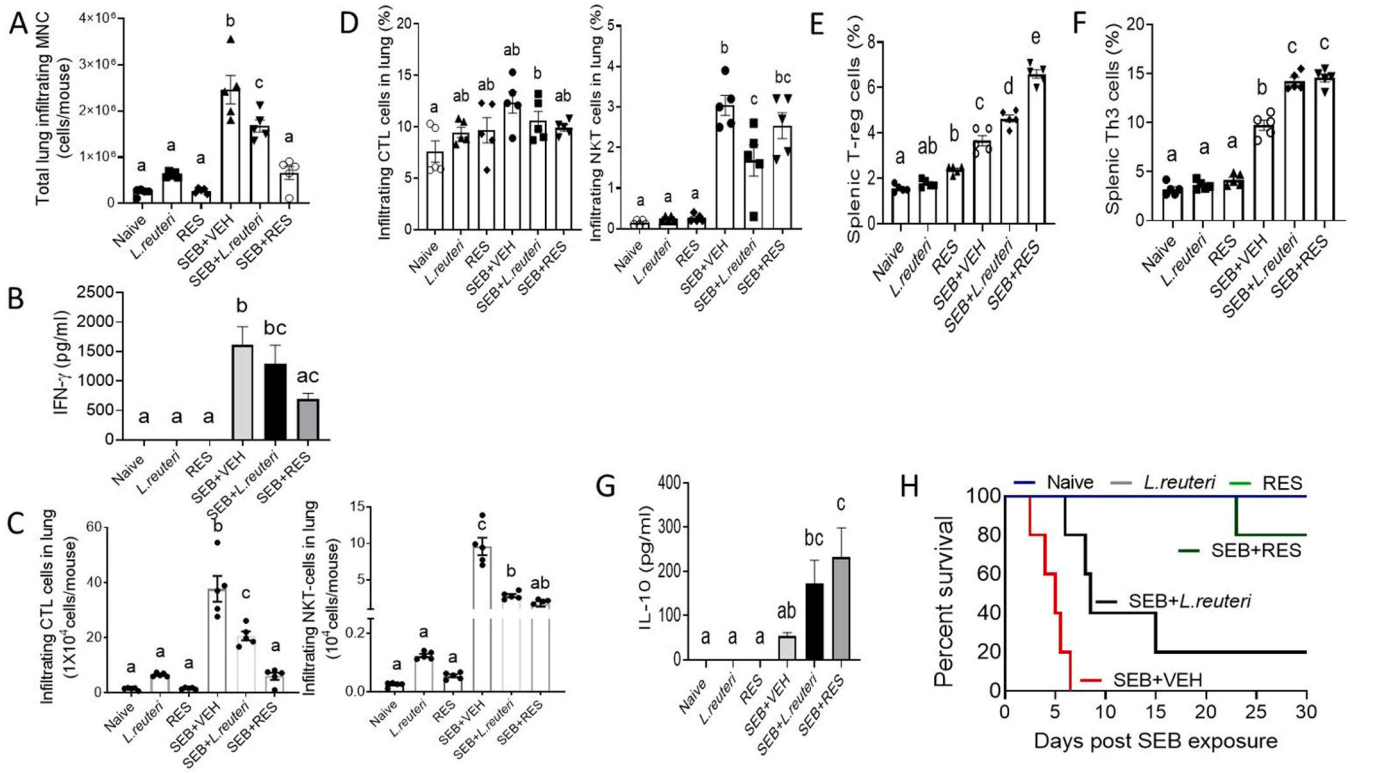

Fig. 4. Administration of RES or Lactobacillus attenuates SEB-induced ARDS. Naïve mice were untreated or treated with RES or *Lactobacillus reuteri*. Also, SEB injected mice were treated with VEH, *L. reuteri* or RES as described in *Materials and methods*. A) Infiltrating mononuclear cells counts in the lungs of SEB-injected mice. ELISA results show the pro-inflammatory (B) and anti-inflammatory cytokines (G) in the sera of experimental mice. C) Absolute number of infiltrating $CD3^+CD8^+$ and NKT cell populations in the lungs. D) Percentage of infiltrating $CD3^+CD8^+$ and NKT cell populations in the lungs. E) Treg populations in spleen gated on $CD3^+CD4^+$. F) T-helper3 population in spleen gated on $CD3^+CD4^+Foxp3^-$. H) Survival rate test for 30 days post-SEB exposure. One-way ANOVA test was used and p-value < 0.05 is considered a significant difference. Log-rank (Mantel-Cox) test was used to compare the survival curves. Bars denote Mean±SEM and any significant differences ($p < 0.05$) are indicated by lowercase letters among groups.

and IL-10 (Fig. 4G), when compared to SEB + VEH group. While SEB + VEH group died with ARDS within ~7 days, 80% of SEB + RES group survived (Fig. 4H) for up to 30 days post SEB exposure, consistent with our previous studies [13]. Using an *in vitro* assay, we also found that pretreatment of splenocytes with RES inhibited the production of inflammatory cytokines such as IFN-γ, IL-1β and IL-17 (Fig. 5A), thereby suggesting that RES was directly acting on immune cells. RES increased the apoptosis rate in the infiltrating mononuclear cells specifically T-cells (Fig. 6A, B) as well as significantly protected the alveolar epithelial barrier integrity from the deleterious effects of SEB-activated immunocytes (Fig. 6C). The gating strategy for various cells stained and analyzed using flow cytometry has been shown in Fig. 1. Together, these data suggested that RES treatment alters the microbiota in the lungs of SEB-treated mice, specifically increasing the abundance of phylum Actinobacteria and species *L. reuteri* and that these changes were associated with suppression of inflammation, and mortality induced by SEB.

3.3. Role of L. reuteri in amelioration of ARDS

Because we found that bacterial species *L. reuteri* was significantly induced in the gut and lungs after RES treatment in SEB-exposed mice (Figs. 2 and 3), we examined the role of *L. reuteri* in the attenuation of SEB-induced ARDS. Similar to the effect of RES, flow cytometric analysis showed that the administration of *L. reuteri* significantly reduced the number of lung-infiltrating MNCs (Fig. 4A); a decrease in the numbers of CD8+ cytotoxic T lymphocytes (CTL) and NKT (Fig. 4C) but not in the percentage (Fig. 4D); an increase in the percentages of Tregs and Th3 cells (Fig. 4E, F); and an increase in serum IL-10 (Fig. 4G). Co-culture of spleen cells with *L. reuteri* followed by SEB activation led to inhibition in the production of IFN-γ, IL-17 and IL-1β but an increase in the production of IL-10 (Fig. 5B). Importantly, when *L. reuteri* was administered into SEB-exposed mice, the mice survived for a longer period and 20% survived for more than 30 days (Fig. 4H). Together, these results demonstrated that administration of *L. reuteri* suppresses inflammatory pathways induced by SEB in the lungs and prevents ARDS although it was not as effective as RES. Nonetheless, these data suggested that RES-mediated suppression of inflammation and ARDS may result, at least in part, from induction of *L. reuteri.*

3.4. CMT to validate the roles of RES and L. reuteri in the amelioration of SEB-mediated ARDS

While we noted that treatment of SEB-immunized mice with RES or *L. reuteri* was associated with alterations in the microbiota and decreased inflammation in the lungs and mortality, it was not clear if this was just an association or actually played a role in suppressing inflammation. In order to confirm the role of microbiota changes induced by RES and *L. reuteri* in the regulation of SEB-mediated attenuation of inflammation, we performed CMT experiments. To that end, donor mice received vehicle, RES, *L. reuteri*, SEB + VEH or SEB + RES. ABX-treated mice were used as the recipients of CMT and received the dual doses of SEB administration after CMT. Metagenomic profiling by pyrosequencing of 16S rRNA gene showed that the abundance of *Lactobacillus spp.* significantly increased in the colon microbiota of recipient mice that received CMT from SEB + RES-treated donor mice (Fig. 7A). However, Firmicutes and Bacilli were the most abundant bacterial species in the colon microbiota of mice that received CMT from *L. reuteri*-treated donors (Fig. 7A). The levels of propionic acid and butyric acid increased

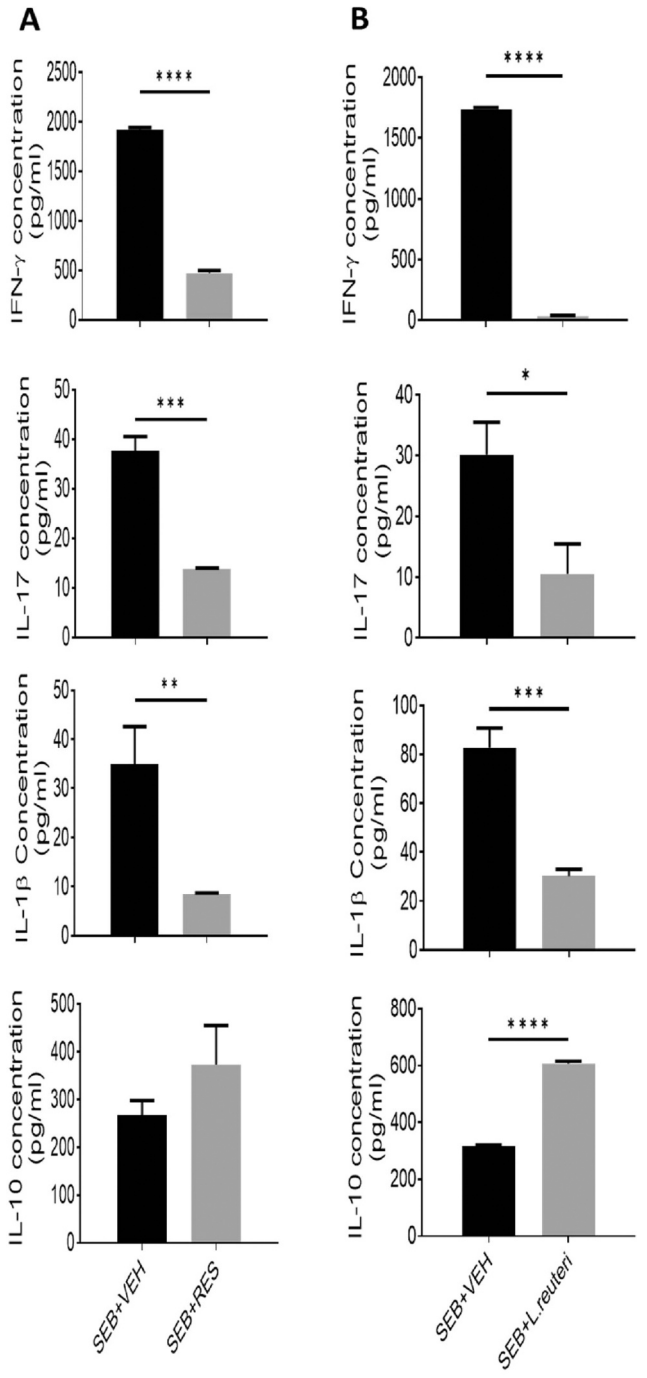

Fig. 5. Effect of RES or *L. reuteri* on the induction of inflammatory cytokines in vitro. Naïve splenocytes were harvested and pre-treated for 1 h with either 50uM RES or *L. reuteri* at a ratios of 1:5 (splenocytes: *L. reuteri)* prior to activation of these cells with 1 μg/ml SEB for 48 h. ELISA was performed to measure IFN-γ, IL-β, IL-17 and IL-10 cytokine levels on supernatants collected 48 h post-SEB activation from, A) RES-pretreated cells. B) *L. reuteri* co-cultured cells. Student's t-test was used and p-value < 0.05 is considered significant difference. *$p < 0.05$, **$p < 0.01$, ***$p < 0.001$ and ****$p < 0.0001$.

significantly in the colon of mice that received CMT from RES- or *L. reuteri*-treated donors (Fig. 7B). The abundance of *L. reuteri* significantly increased in the colon microbiota of recipient mice that received CMT from *L. reuteri*-treated or SEB + RES-treated donor mice (Fig. 7C). In addition, the total number of lung-infiltrating MNCs (Fig. 7D) and the percentage of Th1 cells in the lungs and spleen (Fig. 7E and F), NKT (Fig. 7G) and Th17 cells (Fig. 7H) decreased significantly in the mice received CMT from SEB + RES- or *L. reuteri*-treated donors. Furthermore, the recipient mice showed increased survival rates after CMT from RES, SEB + RES or *L. reuteri*-treated donors (Fig. 7I). These data suggested that both RES-mediated alterations in the microbiota as well as *L. reuteri* administration play, at least in part, a role in suppressing SEB-mediated inflammation, and protection of mice from SEB-mediated lethality.

4. Discussion

Recent studies have shown that gut microbiota may play an important role in health and disease including cardiovascular and immunological disorders [15, 37, 38]. However, there is very limited data on the role of gut microbiota in ARDS pathogenesis [22,39]. Our analysis in the current study showed that there were obvious differences in the compositions of colonic microbiota between naïve mice and SEB-induced ARDS mice (Fig. 2A). Particularly, we noted that the abundance of *Lactobacillus reuteri* significantly increased in colon microbiota in SEB + RES group when compared to SEB + VEH group (Fig. 2G). It should be noted that we also observed significant increase in *Lactobacillus reuteri* in SEB + VEH group when compared to naïve animals. This combined with the observation that *Lactobacillus reuteri* was inducing anti-inflammatory effects suggests that the increase of *Lactobacillus reuteri* in SEB + VEH group may constitute the response of the host aimed at suppressing the inflammation triggered by SEB. Moreover, RES further enhances this effect by inducing even higher levels of *Lactobacillus reuteri.* It was also noted that short chain fatty acids (SCFAs) such as iso-butyric acid and butyric acid significantly decreased in the colon of SEB + VEH group when compared to naïve mice while in SEB + RES group, iso-butyric acid significantly increased when compared to SEB + VEH group (Fig. 2H).

Lung microbiota may also be involved in the regulation of human health and disease such as asthma [18]. However, the role of lung microbiota in the regulation of ARDS pathogenesis has not been studied previously. Our studies found that the biomass of lung microbiota in SEB + VEH treated mice significantly increased when compared to naïve mice (Fig. 3B). Also, the composition of lung microbiota in SEB + VEH group was significantly different from those in seen in naïve mice (Fig. 3A). Proteobacteria phylum and *Propionibacterium acnes* species were dominant in lung microbiota from SEB + VEH group when compared to naïve mice (Fig. 3E). Interestingly we found that SEB-injected mice treated with RES or VEH had no influence on the abundance of Bacteroidetes phylum in the lung or colon. However, RES-treatment enriched the lung and colon commensal communities with beneficial bacteria, such as *Lactobacillus reuteri*, probably by protecting this bacterium from the oxidative stress initiated by immune cells [40]. These data suggested that SEB exposure alters the lung microbiota while the RES revering these changes.

Our previous studies revealed that RES could ameliorate ARDS in mice [12,13]. It has been shown that RES can also modulate gut microbiota [23, 41, 42]. However, whether RES-mediated alterations in the microbiota has any role in the severity of ARDS is not known. We addressed that in the current study and we found that RES could significantly increase the bacterial biomass in colon from SEB-treated mice (Fig. 2B). Also, SEB + RES group showed significant changes in the composition of gut microbiota (Fig. 2A). Specifically, SEB + RES group showed increased abundance of phylum Tenericutes (Fig. 2E), and increased abundance of *Lactobacillus spp.* such as *Lactobacillus reuteri* in colon when compared to SEB + VEH group (Fig. 2F and G). In addition, RES increased the production of SCFA, particularly iso-butyric acids (Fig. 2H). Our studies suggested that RES could modulate gut microbiota in colon, increase the abundance of *Lactobacillus spp.* such as *Lactobacillus reuteri* in gut microbiota and thus ameliorate ARDS.

There are no reports available thus far understanding of role of RES in the regulation of lung microbiota. Our studies discovered that RES significantly enlarged the diversity of lung microbiota in SEB-injected

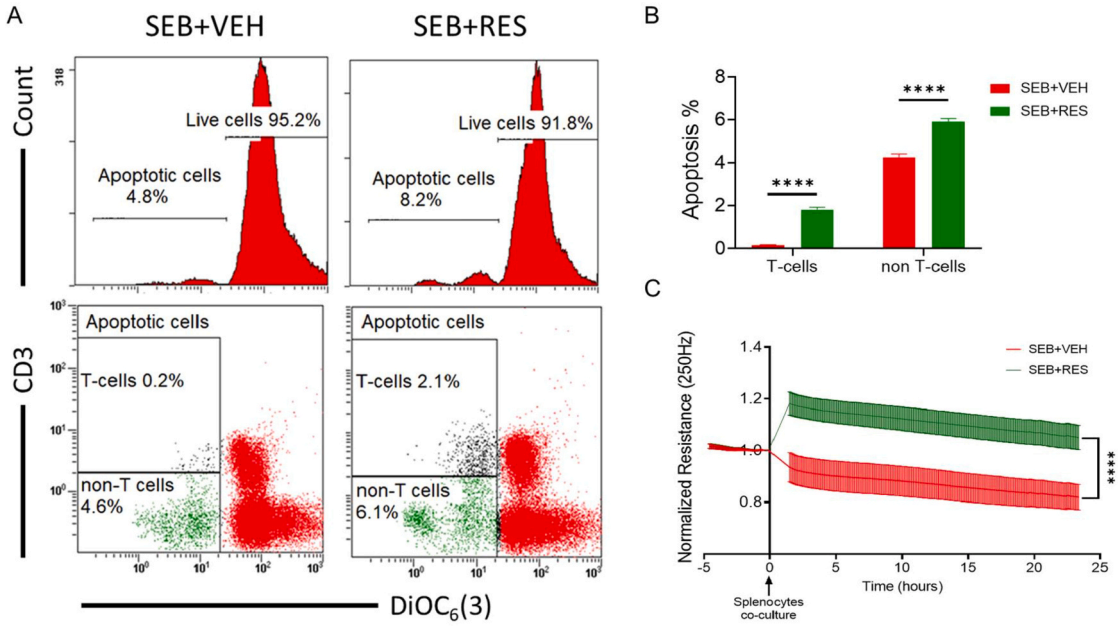

Fig. 6. RES administration increases the apoptosis of effector immune cells and protects the mucosal barrier. Lung-infiltrating mononuclear cells were isolated from the SEB-injected mice treated with RES or VEH and stained with $DiOC_6$ [3] dye to study apoptosis. (A) Shows a representative experiment and B) shows statistical analysis of multiple samples. (C) Alveolar epithelial cells type II (MLE15) was cultured to form monolayer cells before adding SEB-activated splenocytes pre-treated with RES or VEH to evaluate the influence of the inflammatory process on the integrity of the mucosal barrier. Student's t-test was used for B and Mann-Whitney test was used for statistical differences in the curve of barrier function (C). p-value < 0.05 is considered significant difference. ****$p < 0.0001$.

mice (Fig. 3C) and increased the abundance of phylum Actinobacteria and species *L. reuteri* (Fig. 3E, F).

SEB significantly increased Proteobacteria phylum and *Propionibacterium acnes* species in lung microbiota (Fig. 3E). Proteobacteria constitute one of the major phyla of Gram-negative bacteria, composed of a wide variety of pathogenic genera [43]. *Propionibacterium acnes*, a Gram-positive bacterium, is a harmful pathogenic species, which is involved in human diseases [44]. Thus, SEB may induce the growth of several pathogenic bacteria which in turn may promote ARDS pathogenesis. In contrast, RES treatment increased the abundance of phylum Tenericutes, Actinobacteria, and genus *Lactobacillus spp.* such as *Lactobacillus reuteri* in colon from SEB-exposed mice (Figs. 2E–G and 3E and F). The phylum Tenericutes consists of Gram–negative bacteria that play a role in degrading recalcitrant carbon sources in the stomach, and protect the host intestine from invading viruses [45–47]. Actinobacteria is a phylum of Gram-positive bacteria, found both as commensals and terrestrial, known for many beneficial effects. The bacteria in Actinobacteria phylum are the producers of many bioactive metabolites such as antibiotics, which are useful to humans in medicine [48–50]. The genus *Lactobacillus* consists of Gram-positive bacteria, and shows a symbiotic relationship with the human body because they protect the host against potential pathogen invasion and the host provides a source of nutrients for them [51,52].

It is interesting to notice that RES could increase the abundance of *Lactobacillus reuteri* in both gut and lung microbiota from SEB-exposed mice (Figs. 2F, 2G and 3E). RES has been shown to protect *L. reuteri* against protein carbonylation potentially through direct scavenging of reactive oxygen species [40]. *L. reuteri* is a well-known probiotic bacterium and exists in different organs and tissues in humans [53]. It has been reported that *L. reuteri* could produce antimicrobial molecules, and thus inhibit the colonization of pathogenic microbes [54]. *L. reuteri* can inhibit the production of pro-inflammatory cytokines, increase the development and function of Tregs, and thus have an immunosuppressive and regulatory function [55–57]. Our *in vitro* studies found that *L. reuteri* could inhibit the production of IFN-γ, and increase the production of IL-10 (Fig. 5B), while *in vivo*, transfer of *L. reuteri* increased IL-10 (Fig. 4G) but not significantly alter IFN-γ in the sera of SEB administered mice (Fig. 4B). *L. reuteri* also significantly decreased the total number of infiltrating MNCs in the lungs of SEB-treated mice (Fig. 4A) and increased the percentages of Tregs and Th3 in the spleens (Fig. 4E, F). In addition, *L. reuteri* significantly decreased the effector $CD3^+CD8^+$ cells and NKT cells in the lung-infiltrating MNCs from SEB-induced ARDS mice (Fig. 4C). These data together indicated that *L. reuteri* promotes attenuation of SEB-mediated inflammation in the lungs. The importance of microbiota specifically *L. reuteri* in the attenuation of SEB-mediated lung inflammation, ARDS, and mortality was conclusively shown in this study using CMT experiments in which RES-induced microbiota or *L. reuteri* transfer into recipient mice led to attenuation of SEB-mediated toxicity.

As stated, *L. reuteri* could inhibit the production of pro-inflammatory cytokines and increase the development of Tregs. However, the molecular mechanisms through which *L. reuteri* mediates anti-inflammatory properties in ARDS remain to be established. Other investigations reported that *L. reuteri* could activate the Wnt/beta-catenin pathway and increase the expression of antimicrobial peptides, which are responsible for the stimulation of intestinal epithelial cell proliferation, protection of intestinal mucosal barrier integrity, maintenance of number of cells expressing Leucine-rich repeat-containing G-protein-coupled receptor (Lgr5) and promotion of Paneth cell differentiation [58]. Besides, *L. reuteri* could modulate gut microbiota, specifically enrich *Lactobacillus spp.* and *Enterococcus spp.*, and thus improve the lung immune environment and suppress asthma [55]. Our analysis revealed that Firmicutes and Bacilli were the most abundant bacterial species in the colon microbiota of mice that received CMT from *L. reuteri*-treated donors (Fig. 7A), suggesting that *L. reuteri* could enrich Firmicutes and Bacilli species in SEB-injected mice. The results suggested that *L. reuteri* may not only exert immunosuppressive function, but also promote beneficial gut microbiota, thereby providing beneficial effects.

In summary, the current study demonstrates that RES exerts anti-inflammatory properties and attenuates SEB-mediated ARDS and mortality by, at least in part, triggering alterations in microbiota in the lungs and the gut, especially through the induction of beneficial bacteria such

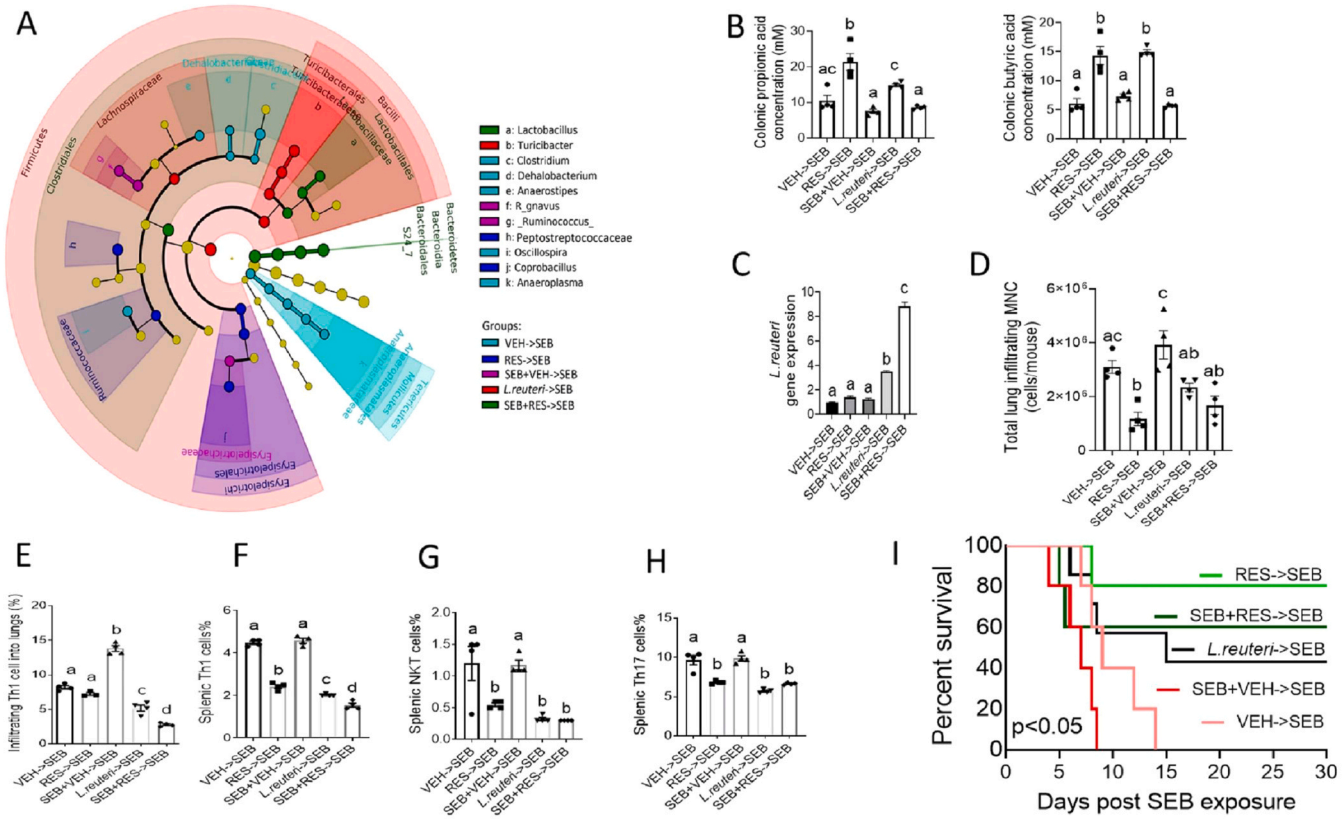

Fig. 7. Effect of CMT from mice treated with RES or *L. reuteri* on SEB-mediated ARDS. Recipient mice were pre-treated with extensive regimen of 8 antibiotics (ABX) for four weeks followed by CMT from RES, VEH, SEB + RES, SEB + VEH donors or *L. reuteri,* and then exposed to SEB, as detailed in Methods. The various groups are represented as follows: CMT from Vehicle treated mice into ABX mice followed by SEB (VEH→SEB), CMT from RES treated mice into ABX mice followed by SEB (RES→SEB), CMT from SEB + VEH treated mice into ABX mice followed by SEB (SEB + VEH→SEB), *L. reuteri* transfer into ABX mice followed by SEB (*L. Reuteri* →SEB), and CMT from SEB + RES treated mice into ABX mice followed by SEB (SEB + RES→SEB). A) Cladogram shows the least significant discriminative changes in gut microbiota amongst various groups. B) Gut content assayed for SCFA including propionic and butyric acids. C) qPCR quantification of *L. reuteri* gene expression in bacterial DNA isolated from the gut. D) Infiltrating mononuclear cells (MNCs) counts in lung tissue. E-H) Flow cytometry results showing percentages of: E) Th1 in lungs. F) Th1 in the spleen G) NKT in the spleen and H) Th17 in the spleen. I) Survival rate observed for 30 days post-SEB exposure. One-way ANOVA test was used. Log-rank (Mantel-Cox) test was used to compare the survival curves. Bars denote Mean ± SEM and any significant differences ($p < 0.05$) are indicated by lowercase letters among groups.

as *L. reuteri* and increased the apoptosis rate in effector immune cells which probably led to an increase in the resistance of alveolar barrier against leaking the inter-alveolar bacteria toward pulmonary interstitial tissue. This was conclusively shown using CMT experiments in which transfer of RES-induced microbiota or *L. reuteri* transfer into recipient mice led to attenuation of SEB-mediated inflammation in the lungs and mortality.

5. Conclusion

Inhalation of SEB is known to induce proinflammatory cytokine storm that leads to weakening of the mucosal barrier, causing microbial dysbiosis and inducing pathogenic bugs into the interstitial tissue then the bacteremia could happen and increase the severity of ARDS which is one of the complications seen in COVID-19 patients. Resveratrol treatment has reversed this dysbiosis and increase enrichments of beneficial bacteria like *Lactobacillus spp.* in the lung and gut from one side. On the other hand, resveratrol was able to directly ameliorate the immune response against SEB and prevent the production of cytokine storm or at least in part by increasing the abundance of beneficial bacteria.

CRediT authorship contribution statement

Hasan Alghetaa: Writing - original draft, Writing - review & editing, Designed research studies, Experimentation and data acquisition, Performing experimnets, Data analysis. **Amira Mohammed:** Designed research studies, Experimentation and data acquisition, Writing - review & editing, Data analysis, Performing experiments**. Juhua Zhou:** Writing - review & editing. **Mitzi Nagarkatti:** Writing - review & editing, Funding acquisition, Resources, Supervision, Designed research studies. **Prakash Nagarkatti:** Writing - review & editing, Funding acquisition, Resources, Supervision, Designed research studies.

Acknowledgements

Special thanks to Dr. Jeffrey A. Whitsett from Perinatal Institute, Cincinnati Children's Hospital Medical Center, Department of Pediatrics, Division of Neonatology, Perinatal and Pulmonary Biology, Cincinnati, Ohio, for providing us with the MLE15 cell line. These studies were supported in part by NIH grants: P01AT003961, P20GM103641, R01AT006888, R01ES030144, and R01AI123947 to PN and MN. Iraqi MoHESR Scholarship to AM.

Conflict of Interest

The authors declare no conflict of interest in this study.

References

[1] E. Fan, D. Brodie, A.S. Slutsky, Acute respiratory distress syndrome: advances in diagnosis and treatment, JAMA 319 (7) (2018) 698–710, https://doi.org/10.1001/jama.2017.21907.

[2] A. Nadeem, N.O. Al-Harbi, S.F. Ahmad, M.M. Al-Harbi, A.S. Alhamed, A. S. Alfardan, M.A. Assiri, K.E. Ibrahim, H. Albassam, Blockade of interleukin-2-inducible T-cell kinase signaling attenuates acute lung injury in mice through adjustment of pulmonary Th17/Treg immune responses and reduction of oxidative stress, Int. Immunopharmacol. 83 (2020), 106369, https://doi.org/10.1016/j.intimp.2020.106369.

[3] F. Kong, Y. Sun, W. Song, Y. Zhou, S. Zhu, MiR-216a alleviates LPS-induced acute lung injury via regulating JAK2/STAT3 and NF-kappaB signaling, Hum. Cell. 33 (1) (2020) 67–78, https://doi.org/10.1007/s13577-019-00289-7.

[4] N. Qiu, X. Xu, Y. He, LncRNA TUG1 alleviates sepsis-induced acute lung injury by targeting miR-34b-5p/GAB1, BMC Pulm. Med. 20 (1) (2020) 49, https://doi.org/10.1186/s12890-020-1084-3.

[5] S.A. Rieder, P. Nagarkatti, M. Nagarkatti, CD1d-independent activation of invariant natural killer T cells by staphylococcal enterotoxin B through major histocompatibility complex class II/T cell receptor interaction results in acute lung injury, Infect. Immun. 79 (8) (2011) 3141–3148, https://doi.org/10.1128/IAI.00177-11.

[6] R.J. McKallip, M. Fisher, U. Gunthert, A.K. Szakal, P.S. Nagarkatti, M. Nagarkatti, Role of CD44 and its v7 isoform in staphylococcal enterotoxin B-induced toxic shock: CD44 deficiency on hepatic mononuclear cells leads to reduced activation-induced apoptosis that results in increased liver damage, Infect. Immun. 73 (1) (2005) 50–61, https://doi.org/10.1128/IAI.73.1.50-61.2005.

[7] A. Mohammed, H. Alghetaa, K. Miranda, K. Wilson, N.P. Singh, G. Cai, N. Putluri, P. Nagarkatti, M. Nagarkatti, Δ9-Tetrahydrocannabinol prevents mortality from acute respiratory distress syndrome through the induction of apoptosis in immune cells, leading to cytokine storm suppression, Int. J. Mol. Sci. 21 (17) (2020) 6244, https://doi.org/10.3390/ijms21176244.

[8] B. Salehi, A.P. Mishra, M. Nigam, B. Sener, M. Kilic, M. Sharifi-Rad, P.V.T. Fokou, N. Martins, J. Sharifi-Rad, Resveratrol: a double-edged sword in health benefits, Biomedicines 6 (3) (2018) 91, https://doi.org/10.3390/biomedicines6030091.

[9] J.M. Sales, A.V. Resurreccion, Resveratrol in peanuts, Crit. Rev. Food Sci. Nutr. 54 (6) (2014) 734–770, https://doi.org/10.1080/10408398.2011.606928.

[10] M. Chen, Q. Fu, X. Song, A. Muhammad, R. Jia, Y. Zou, L. Yin, L. Li, C. He, G. Ye, C. Lv, X. Liang, J. Huang, M. Cui, Z. Yin, Preparation of resveratrol dry suspension and its immunomodulatory and anti-inflammatory activity in mice, Pharm. Biol. 58 (1) (2020) 8–15, https://doi.org/10.1080/13880209.2019.1699123.

[11] X. Meng, J. Zhou, C.N. Zhao, R.Y. Gan, H.B. Li, Health benefits and molecular mechanisms of resveratrol: a narrative review, Foods 9 (3) (2020) 340, https://doi.org/10.3390/foods9030340.

[12] S.A. Rieder, P. Nagarkatti, M. Nagarkatti, Multiple anti-inflammatory pathways triggered by resveratrol lead to amelioration of staphylococcal enterotoxin B-induced lung injury, Br. J. Pharmacol. 167 (6) (2012) 1244–1258, https://doi.org/10.1111/j.1476-5381.2012.02063.x.

[13] H. Alghetaa, A. Mohammed, M. Sultan, P. Busbee, A. Murphy, S. Chatterjee, M. Nagarkatti, P. Nagarkatti, Resveratrol protects mice against SEB-induced acute lung injury and mortality by miR-193a modulation that targets TGF-beta signalling, J. Cell Mol. Med 22 (5) (2018) 2644–2655, https://doi.org/10.1111/jcmm.13542.

[14] E. Alharris, H. Alghetaa, R. Seth, S. Chatterjee, N.P. Singh, M. Nagarkatti, P. Nagarkatti, Resveratrol attenuates allergic asthma and associated inflammation in the lungs through regulation of miRNA-34a that targets FoxP3 in mice, Front Immunol. 9 (2018) 2992, https://doi.org/10.3389/fimmu.2018.02992.

[15] A. Gupta, S. Saha, S. Khanna, Therapies to modulate gut microbiota: past, present and future, World J. Gastroenterol. 26 (8) (2020) 777–788, https://doi.org/10.3748/wjg.v26.i8.777.

[16] A.J. Waldman, E.P. Balskus, The human microbiota, infectious disease, and global health: challenges and opportunities, ACS Infect. Dis. 4 (1) (2018) 14–26, https://doi.org/10.1021/acsinfecdis.7b00232.

[17] A. Mohammed, H. Alghetaa, J. Zhou, S. Chatterjee, P. Nagarkatti, M. Nagarkatti, Protective effects of Δ9-tetrahydrocannabinol against enterotoxin-induced acute respiratory distress syndrome are mediated by modulation of microbiota, Br. J. Pharmacol. 177 (22) (2020) 5078–5095, https://doi.org/10.1111/bph.15226.

[18] W. Barcik, R.C.T. Boutin, M. Sokolowska, B.B. Finlay, The role of lung and gut microbiota in the pathology of asthma, Immunity 52 (2) (2020) 241–255, https://doi.org/10.1016/j.immuni.2020.01.007.

[19] G. Fitzgibbon, K.H.G. Mills, The microbiota and immune-mediated diseases: opportunities for therapeutic intervention, Eur. J. Immunol. 50 (3) (2020) 326–337, https://doi.org/10.1002/eji.201948322.

[20] M. Salameh, Z. Burney, N. Mhaimeed, I. Laswi, N.A. Yousri, G. Bendriss, D. Zakaria, The role of gut microbiota in atopic asthma and allergy, implications in the understanding of disease pathogenesis, Epub 2019/12/04, Scand. J. Immunol. 91 (3) (2020), e12855, https://doi.org/10.1111/sji.12855.

[21] R. Kapur, M. Kim, J. Rebetz, B. Hallstrom, J.T. Bjorkman, A. Takabe-French, N. Kim, J. Liu, S. Shanmugabhavananthan, S. Milosevic, M.J. McVey, E.R. Speck, J. W. Semple, Gastrointestinal microbiota contributes to the development of murine transfusion-related acute lung injury, Blood Adv. 2 (13) (2018) 1651–1663, https://doi.org/10.1182/bloodadvances.2018018903.

[22] B. Li, G.F. Yin, Y.L. Wang, Y.M. Tan, C.L. Huang, X.M. Fan, Impact of fecal microbiota transplantation on TGF-β1/Smads/ERK signaling pathway of endotoxic acute lung injury in rats, 3 Biotech 10 (2) (2020) 52, https://doi.org/10.1007/s13205-020-2062-4.

[23] H.R. Alrafas, P.B. Busbee, M. Nagarkatti, P.S. Nagarkatti, Resveratrol modulates the gut microbiota to prevent murine colitis development through induction of Tregs and suppression of Th17 cells, J. Leukoc. Biol. 106 (2) (2019) 467–480, https://doi.org/10.1002/JLB.3A1218-476RR.

[24] F. Li, Y. Han, X. Cai, M. Gu, J. Sun, C. Qi, T. Goulette, M. Song, Z. Li, H. Xiao, Dietary resveratrol attenuated colitis and modulated gut microbiota in dextran sulfate sodium-treated mice, Food Funct. 11 (1) (2020) 1063–1073, https://doi.org/10.1039/c9fo01519a.

[25] B.C. Fries, A.K. Varshney, Bacterial toxins-staphylococcal enterotoxin B, Microbiol. Spectr. 1 (2) (2015) 303–318, https://doi.org/10.1128/microbiolspec.AID-0002-2012.

[26] L.M. Huzella, M.J. Buckley, D.A. Alves, B.G. Stiles, T. Krakauer, Central roles for IL-2 and MCP-1 following intranasal exposure to SEB: a new mouse model, Res. Vet. Sci. 86 (2) (2009) 241–247, https://doi.org/10.1016/j.rvsc.2008.07.020.

[27] A.I. Saeed, S.A. Rieder, R.L. Price, J. Barker, P. Nagarkatti, M. Nagarkatti, Acute lung injury induced by Staphylococcal enterotoxin B: disruption of terminal vessels as a mechanism of induction of vascular leak, Microsc. Microanal. 18 (3) (2012) 445–452, https://doi.org/10.1017/S1431927612000190.

[28] L. Hu, Z. Chen, L. Li, Z. Jiang, L. Zhu, Resveratrol decreases CD45(+) CD206(-) subtype macrophages in LPS-induced murine acute lung injury by SOCS3 signalling pathway, J. Cell Mol. Med. 23 (12) (2019) 8101–8113, https://doi.org/10.1111/jcmm.14680 (PubMed PMID: 31559687; PMCID: PMC6850919).

[30] Z.Z. Al-Ghezi, P.B. Busbee, H. Alghetaa, P.S. Nagarkatti, M. Nagarkatti, Combination of cannabinoids, delta-9-tetrahydrocannabinol (THC) and cannabidiol (CBD), mitigates experimental autoimmune encephalomyelitis (EAE) by altering the gut microbiome, Brain Behav. Immun. 82 (2019) 25–35, https://doi.org/10.1016/j.bbi.2019.07.028.

[31] G.B. Huffnagle, R.P. Dickson, N.W. Lukacs, The respiratory tract microbiome and lung inflammation: a two-way street, Mucosal Immunol. 10 (2) (2017) 299–306, https://doi.org/10.1038/mi.2016.108.

[32] A. Klindworth, E. Pruesse, T. Schweer, J. Peplies, C. Quast, M. Horn, F.O. Glockner, Evaluation of general 16S ribosomal RNA gene PCR primers for classical and next-generation sequencing-based diversity studies, Nucleic Acids Res. 41 (1) (2013), e1, https://doi.org/10.1093/nar/gks808.

[33] N. Weber, D. Liou, J. Dommer, P. MacMenamin, M. Quinones, I. Misner, A.J. Oler, J. Wan, L. Kim, M. Coakley McCarthy, S. Ezeji, K. Noble, D.E. Hurt, Nephele: a cloud platform for simplified, standardized and reproducible microbiome data analysis, Bioinformatics 34 (8) (2018) 1411–1413, https://doi.org/10.1093/bioinformatics/btx617.

[34] G. Li, C. Xie, S. Lu, R.G. Nichols, Y. Tian, L. Li, D. Patel, Y. Ma, C.N. Brocker, T. Yan, K.W. Krausz, R. Xiang, O. Gavrilova, A.D. Patterson, F.J. Gonzalez, Intermittent fasting promotes white adipose browning and decreases obesity by shaping the gut microbiota, Cell Metab. 26 (4) (2017) 672–685.e4, https://doi.org/10.1016/j.cmet.2017.08.019.

[35] A. Mohammed, H. Alghetaa, M. Sultan, N.P. Singh, P. Nagarkatti, M. Nagarkatti, Administration of Δ9-tetrahydrocannabinol (THC) post-staphylococcal enterotoxin B exposure protects mice from acute respiratory distress syndrome and toxicity, Front Pharmacol. 11 (2020) 893, https://doi.org/10.3389/fphar.2020.00893.

[36] E. Afgan, D. Baker, B. Batut, M. van den Beek, D. Bouvier, M. Cech, J. Chilton, D. Clements, N. Coraor, B.A. Gruning, A. Guerler, J. Hillman-Jackson, S. Hiltemann, V. Jalili, H. Rasche, N. Soranzo, J. Goecks, J. Taylor, A. Nekrutenko, D. Blankenberg, The Galaxy platform for accessible, reproducible and collaborative biomedical analyses: 2018 update, Nucleic Acids Res. 46 (W1) (2018) W537–W544, https://doi.org/10.1093/nar/gky379.

[37] P. Nie, Z. Li, Y. Wang, Y. Zhang, M. Zhao, J. Luo, S. Du, Z. Deng, J. Chen, S. Chen, L. Wang, Gut microbiome interventions in human health and diseases, Med. Res. Rev. 39 (6) (2019) 2286–2313, https://doi.org/10.1002/med.21584.

[38] H. Yu, Y.N. Ni, Z.A. Liang, B.M. Liang, Y. Wang, The effect of aspirin in preventing the acute respiratory distress syndrome/acute lung injury: a meta-analysis, Am. J. Emerg. Med. 36 (8) (2018) 1486–1491, https://doi.org/10.1016/j.ajem.2018.05.017.

[39] S. Chen, H. Xu, P. Ye, C. Wu, X. Ding, H. Zhang, Y. Zou, J. Zhao, S. Le, J. Wu, J. Xia, Trametinib alleviates lipopolysaccharide-induced acute lung injury by inhibiting the MEK-ERK-Egr-1 pathway, Int. Immunopharmacol. 80 (2020), 106152, https://doi.org/10.1016/j.intimp.2019.106152.

[40] N.O. Arcanjo, M.J. Andrade, P. Padilla, A. Rodriguez, M.S. Madruga, M. Estevez, Resveratrol protects Lactobacillus reuteri against H2O2- induced oxidative stress and stimulates antioxidant defenses through upregulation of the dhaT gene, Free Radic. Biol. Med. 135 (2019) 38–45, https://doi.org/10.1016/j.freeradbiomed.2019.02.023.

[41] A. Chaplin, C. Carpene, J. Mercader, Resveratrol, metabolic syndrome, and gut microbiota, Nutrients 10 (11) (2018) 1651, https://doi.org/10.3390/nu10111651.

[42] P. Wang, D. Li, W. Ke, D. Liang, X. Hu, F. Chen, Resveratrol-induced gut microbiota reduces obesity in high-fat diet-fed mice, Int. J. Obes. 44 (1) (2020) 213–225, https://doi.org/10.1038/s41366-019-0332-1.

[43] Z. Kang, M. Lu, M. Jiang, D. Zhou, H. Huang, Proteobacteria acts as a pathogenic risk-factor for chronic abdominal pain and diarrhea in post-cholecystectomy syndrome patients: a gut microbiome metabolomics study, Med. Sci. Monit. Int. Med. J. Exp. Clin. Res. 25 (2019) 7312–7320, https://doi.org/10.12659/MSM.915984.

[44] M.E. Portillo, S. Corvec, O. Borens, A. Trampuz, Propionibacterium acnes: an underestimated pathogen in implant-associated infections, BioMed Res. Int. 2013 (2013) 1–10, https://doi.org/10.1155/2013/804391.

[45] Y. Wang, U. Stingl, F. Anton-Erxleben, S. Geisler, A. Brune, M. Zimmer, "Candidatus hepatoplasma crinochetorum," a new, stalk-forming lineage of Mollicutes colonizing the midgut glands of a terrestrial isopod, Appl. Environ.

Microbiol. 70 (10) (2004) 6166–6172, https://doi.org/10.1128/AEM.70.10.6166-6172.2004.
[46] Y. Wang, J.M. Huang, S.L. Wang, Z.M. Gao, A.Q. Zhang, A. Danchin, L.S. He, Genomic characterization of symbiotic mycoplasmas from the stomach of deep-sea isopod bathynomus sp, Environ. Microbiol. 18 (8) (2016) 2646–2659, https://doi.org/10.1111/1462-2920.13411.
[47] L.S. He, P.W. Zhang, J.M. Huang, F.C. Zhu, A. Danchin, Y. Wang, The enigmatic genome of an obligate ancient spiroplasma symbiont in a hadal holothurian, Appl. Environ. Microbiol. 84 (1) (2018), https://doi.org/10.1128/AEM.01965-17.
[48] A.A. Elbendary, A.M. Hessain, M.D. El-Hariri, A.A. Seida, I.M. Moussa, A. S. Mubarak, S.A. Kabli, H.A. Hemeg, J.K. El Jakee, Isolation of antimicrobial producing Actinobacteria from soil samples, Saudi J. Biol. Sci. 25 (1) (2018) 44–46, https://doi.org/10.1016/j.sjbs.2017.05.003.
[49] E.A. Barka, P. Vatsa, L. Sanchez, N. Gaveau-Vaillant, C. Jacquard, J.P. Meier-Kolthoff, H.P. Klenk, C. Clement, Y. Ouhdouch, G.P. van Wezel, Taxonomy, physiology, and natural products of Actinobacteria, Microbiol. Mol. Biol. Rev. 80 (1) (2016) 1–43, https://doi.org/10.1128/MMBR.00019-15.
[50] N. Kasanah, T. Triyanto, Bioactivities of halometabolites from marine Actinobacteria, Biomolecules 9 (6) (2019) 225, https://doi.org/10.3390/biom9060225.
[51] R. Martin, S. Miquel, J. Ulmer, N. Kechaou, P. Langella, L.G. Bermudez-Humaran, Role of commensal and probiotic bacteria in human health: a focus on inflammatory bowel disease, Microb. Cell Factor. 12 (2013) 71, https://doi.org/10.1186/1475-2859-12-71.
[52] G.R. Lewin, C. Carlos, M.G. Chevrette, H.A. Horn, B.R. McDonald, R.J. Stankey, B. G. Fox, C.R. Currie, Evolution and ecology of Actinobacteria and their bioenergy applications, Annu. Rev. Microbiol. 70 (2016) 235–254, https://doi.org/10.1146/annurev-micro-102215-095748.
[53] Q. Mu, V.J. Tavella, X.M. Luo, Role of Lactobacillus reuteri in human health and diseases, Front. Microbiol. 9 (2018) 757, https://doi.org/10.3389/fmicb.2018.00757.
[54] H. Liu, C. Hou, G. Wang, H. Jia, H. Yu, X. Zeng, P.A. Thacker, G. Zhang, S. Qiao, Lactobacillus reuteri I5007 modulates intestinal host defense peptide expression in the model of IPEC-J2 cells and neonatal piglets, Nutrients 9 (6) (2017) 559, https://doi.org/10.3390/nu9060559.
[55] L. Li, Z. Fang, X. Liu, W. Hu, W. Lu, Y.K. Lee, J. Zhao, H. Zhang, W. Chen, Lactobacillus reuteri attenuated allergic inflammation induced by HDM in the mouse and modulated gut microbes, PloS One 15 (4) (2020), e0231865, https://doi.org/10.1371/journal.pone.0231865. PubMed PMID: 32315360.
[56] Y. Liu, N.Y. Fatheree, B.M. Dingle, D.Q. Tran, J.M. Rhoads, Lactobacillus reuteri DSM 17938 changes the frequency of Foxp3+ regulatory T cells in the intestine and mesenteric lymph node in experimental necrotizing enterocolitis, PloS One 8 (2) (2013), e56547, https://doi.org/10.1371/journal.pone.0056547.
[57] W.H. Neamah, P.B. Busbee, H. Alghetaa, O.A. Abdulla, M. Nagarkatti, P. Nagarkatti, AhR activation leads to alterations in the gut microbiome with consequent effect on induction of myeloid derived suppressor cells in a CXCR2-dependent manner, Int. J. Mol. Sci. 21 (24) (2020) 9613, https://doi.org/10.3390/ijms21249613.
[58] H. Wu, S. Xie, J. Miao, Y. Li, Z. Wang, M. Wang, Q. Yu, Lactobacillus reuteri maintains intestinal epithelial regeneration and repairs damaged intestinal mucosa, Gut Microbes 11 (2020) 997–1014, https://doi.org/10.1080/19490976.2020.1734423.